Applied Catalysis B: Environmental 156–157 (2014) 284–292

Contents lists available at ScienceDirect

Applied Catalysis B: Environmental

journal homepage: www.elsevier.com/locate/apcatb

Effect of inorganic ions on the photocatalytic treatment of agro-industrial wastewaters containing imazalil

Dunia E. Santiago*, J. Araña, O. González-Díaz, M.E. Alemán-Dominguez, Andrea C. Acosta-Dacal, C. Fernandez-Rodríguez, J. Pérez-Peña, José M. Doña-Rodríguez

Grupo de Fotocatálisis y Espectroscopía Aplicada al Medioambiente-FEAM (Unidad Asociada al ICMSE, C.S.I.C.), CIDIA-Dpto. de Química, Edificio del Parque Científico Tecnológico, Universidad de Las Palmas de Gran Canaria, Campus Universitario de Tafira, 35017 Las Palmas, Spain

ARTICLE INFO

Article history:
Received 18 December 2013
Received in revised form 8 March 2014
Accepted 11 March 2014
Available online 21 March 2014

Keywords:
Wastewater
Photocatalysis
Imazalil
Banana postharvest
Ions

ABSTRACT

In this work we studied the elimination, mineralization and detoxification of wastewaters from banana postharvest industries, contaminated with the fungicide imazalil, by means of heterogeneous advanced oxidation processes. We compared the activity of the commercial photocatalyst Evonik P25 and the lab-made EST-1023t in the degradation of imazalil in deionized water and in industrial wastewater. Results show an important negative water-matrix effect for wastewater treatment at acidic pH values due, mainly, to the presence of ions adsorbed onto the TiO_2 photocatalyst surface. At pH 7 only bicarbonate anions and bacteria hindered the degradation and mineralization of imazalil. Mineralization of imazalil was completely inhibited by dissolved aluminium in concentrations as low as 5 mg L^{-1}.

1. Introduction

In order to prevent the appearance of postharvest diseases during the transportation and storage of fruits, it is necessary to employ fungicides. Water contaminated with these substances is normally disposed into the sewage system and thus produces a negative environmental impact. Legislations have been established by many countries to control fungicide MRLs (maximum residual levels) in fruits [1,2], as well as fungicide MCLs (maximum contaminant levels) in wastewater [3].

In this study, wastewater samples from a banana producer were analyzed. This producer employs imazalil as postharvest fungicide in order to prevent banana crown rot. In addition, a considerable amount of aluminium sulphate is added to the process to flocculate the dirt particles washed away from the fruit and thus delay the renewal of wash-water [4]. Calcium hydroxide is also added to increase water pH to prevent corrosion of the washing machinery.

Conventional wastewater treatment plants, based on biological treatments, are unable to eliminate certain substances such as fungicides due to the low biodegradability of these pollutants [5,6]. Advanced oxidation techniques, including heterogeneous TiO_2-based photocatalysis, have proved to be an efficient alternative for the degradation of fungicides, including imazalil [7–10]. This technique is based on the production by the photocatalyst of highly reactive oxidizing agents, such as hydroxyl radicals (•OH). However, the presence of inorganic ions in the water matrix has been shown to greatly influence the removal efficiency of target pollutants [11–15].

The objective of this study is the optimization of the removal of imazalil from an industrial wastewater effluent by means of heterogeneous photocatalysis. For this purpose, two TiO_2-based photocatalysts, commercial Evonik P25 and the lab-made EST-1023t photocatalyst, were tested. Both photocatalysts have proven to be efficient in the degradation and mineralization of imazalil in deionized water [10].

The effects of the most abundant ions (Cl^-, SO_4^{2-}, HCO_3^-, Al^{3+} and Ca^{2+}) in the collected wastewater were also studied on an individual basis.

2. Materials and methods

2.1. Reagents/chemicals

The photocatalysts used in the experiments and their properties are shown in Table 1.

The imazalil used was the commercial Fruitgard-IS-7.5. pH was adjusted with diluted H_2SO_4 or HCl and NaOH or $Ca(OH)_2$.

* Corresponding author.
E-mail addresses: dsantiago@proyinves.ulpgc.es, jdona@dqui.ulpgc.es (D.E. Santiago), jdona@dqui.ulpgc.es (J.M. Doña-Rodríguez).

http://dx.doi.org/10.1016/j.apcatb.2014.03.022
0926-3373/

Table 1
Characteristics of the different photocatalysts used in this work [9].

Catalyst	Specific surface area ($m^2\ g^{-1}$)	Anatase/Rutile ratio (%)	Crystallite size (nm)		Band gap (eV)	pH_{pzc}	Particle size (μm)
			Anatase	Rutile			
Evonik P25	52	80/20	22.0	25.0	3.18	6.5	3.9
EST-1023t	13.51	70–80/30–20	62.3	96.1	2.96	6.2	30.1

To study the effect of various inorganic ions, sodium chloride (NaCl), sodium bicarbonate ($NaHCO_3$), sodium sulfate (Na_2SO_4), aluminium sulphate ($Al_2(SO_4)_3{\cdot}18H_2O$) and calcium sulphate ($CaSO_4{\cdot}2H_2O$), from Panreac, were used.

2.2. Analytical determinations

Concentrations of imazalil at different reaction times were HPLC measured according to [10].

Total organic carbon (TOC) and inorganic carbon (IC) were measured using a TOC Shimadzu V-CSN.

Analysis of intermediates was performed with a Varian System consisting of a 212-LC Binary Gradient LC/MS Chromatography Pump fitted with a Prostar 410 HPLC Autosampler and a 320–MS LC/MS/MS system (triple quadrupole) equipped with an electrospray ionization (ESI) interface, according to [10]. Solid-phase extraction using Waters Sep-Pak C18 (500 mg) cartridges was applied to the samples to reduce the salting out effect before chromatographic analysis [16].

Sample toxicity was determined with the MultiTox® *Vibrio fischeri* toxicity test following standard UNE-EN-ISO 11348-3:1998, using an Optocomp I luminometer from MGM Instruments.

Ion Chromatography was used to determine ion concentrations in solution. For this purpose, a DIONEX Ionic Chromatograph equipped with a GP50 gradient pump, ED50 electrochemical detector and an IonPac AS11-HC column (4 × 250 mm) for anions or an IonPac CS12A column (2 × 250 mm) for cations were employed, using a flow rate of 1 mL min^{-1} and aqueous NaOH (30 mM) or 20 mM metasulphonic acid as eluent for anions and cations, respectively.

The FTIR (Fourier Transform Infrared) determinations followed the procedure described in [10].

For dissolved aluminium determinations, a GFAAS (AA 240z Zeeman) graphite furnace atomizer (Varian GTA120) and longitudinal Zeeman-effect background correction were used. A Varian hollow cathode lamp (HCL) was used with wavelength of 396.2 nm. Atomization was held for 2.8 s at 2500 °C. The flowrate of the inert gas (argon) was 0.3 L min^{-1}. This flow was stopped during atomization. The detection and quantification limits for aluminium were 0.35 μg L^{-1} and 1.06 μg L^{-1}, respectively. The adjusted R^2 was 0.9998.

Total suspended solids were measured following standard EN-872, BOD_5 was measured following ISO 5815:1989 using Velp Scientifica BOD Sensor System 10, and COD was determined according to standard ISO 6060:1989 using Velp Scientifica Eco6 Thermoreactor for digestion.

Heterotrophic bacteria were determined using the Heterotrophic Plate Count (HPC) method and R2A as culture media following Standard Methods (9215 C APHA) with incubation at 28 °C for 7 days.

3. Experimental conditions

Degradation tests were performed in 250 mL Pyrex glass batch reactors, filled with 200 mL of the pollutant aqueous solution and 1 g L^{-1} of photocatalyst. Aeration was maintained with an aquarium pump (EOLO AC3000 model: 2.5 W power, 2 L min^{-1} output and pressure >0.02 MPa) and a constant stirring of 450 rpm. A 60 W Philips Solarium HB175 equipped with four 15 W Philips CLEO fluorescent tubes with emission spectrum from 300 to 400 nm (maximum around 365 nm) and with an average irradiation power of about 9 mW was used as UV source in the photodegradation and mineralization studies. The lamp was turned on after establishing the adsorption equilibrium. Samples were taken to monitor the reaction in time intervals of 15 min during the first hour and 30 min thereafter. The samples were filtered using 0.45 μm syringe filters before analysis. The experimental setup is shown in Scheme 1.

The photocatalytic process was studied for initial imazalil concentrations of 50 mg L^{-1}. Studies were carried out in deionized water, in the wastewater sample and, finally, in the presence of each of the main ions found in the wastewater sample to evaluate the interference of each ion on the photocatalytic treatment.

Suspended solids and flocs in wastewater were left to settle and the supernatant, free of turbidity, was filtered through 0.45 μm filters for the experimental assays. In order to evaluate the possible effect of bacteria in the photocatalytic treatment, assays were also performed without the filtering stage.

The data presented in this work were subjected to statistical treatment. The standard errors shown in the Figures were calculated using 95% confidence limits.

4. Results and discussion

4.1. Characterization of industrial water sample

The banana producer that provided wastewater for this study processes 10,000 tn yr^{-1} of banana and generates 63 m^3 $week^{-1}$ wastewater containing imazalil.

The mean main parameters found in the wastewater samples from this company and the MCLs for wastewater disposal [17] and reuse in irrigation [18] in the particular case of Spain are listed in Table 2.

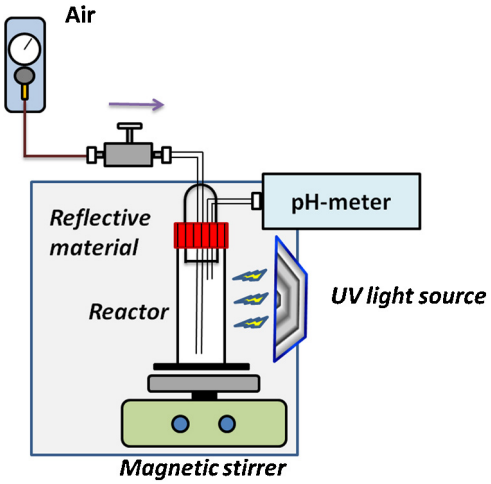

Scheme 1. Experimental setup.

Table 2
Parameters of the wastewater samples recollected from a banana producer and MCLs in Spain.

Parameter	Wastewater sample	MCL for reuse	MCL for disposal[a]
Imazalil (mg L^{-1})	42.35	0.05	0.05
pH	4.34	6.5–8.5	5.5–9.5
BOD_5 (mg L^{-1})	19.7	40	1000
COD (mg L^{-1})	162.86	160	1600
TSS (mg L^{-1})	39	80	1200
Turbidity (NTU)	27.20	1–10	–
Toxicity (% Inh.)	99.14	–	–
TOC (mg L^{-1})	26.67	–	–
Heterotrophic total bacteria (cfu/100 mL)	$2{\cdot}10^4$	<1000[b]	–
SAR (meq L^{-1})	10.09	6	–
Cl^- (mg L^{-1})	80.91	2000	300
S_4^{2-} (mg L^{-1})	287.50	2000	350
NO_3^- (mg L^{-1})	2.09	10	20
HCO_3^- (mg L^{-1})	<18	–	–
Ca^{2+} (mg L^{-1})	17.61	–	–
Mg^{2+} (mg L^{-1})	2.58	–	–
Na^+ (mg L^{-1})	51.20	–	–
K^+ (mg L^{-1})	2.70	–	–
Al^{3+} (mg L^{-1})	4.04	1	2

[a] MCLs for disposal into the sewage system according to the Spanish legislation.
[b] This value must be obtained from the mean of 10 replicates, of which no more than 3 can present > 1000 cfu/100 mL and none of the replicates must contain > 10,000 cfu/100 mL.

As can be seen in Table 2, mean imazalil concentration in the collected wastewater samples was 42.35 mg L^{-1}. Therefore, 50 mg L^{-1} of imazalil was taken as the working concentration.

It can also be seen that COD/BOD5 > 10, which suggests that the wastewater contains mainly non-biodegradable matter.

Although three compounds are authorized in banana postharvest in Spain (imazalil, thiabendazole and pyrethrins) the only fungicide used by the collaborating producer of this study is imazalil, making it the principal contaminant present in the wastewater samples. Though other organic matter may be present from dirt washed away from the fruit in the washing process, the amount in this particular case will be negligible. Many pesticides are authorized in the cultivation of bananas in Spain [19], among which the most common are chlorpyrifos, glyphosate and hexythiazox, and thus the postharvest cleaning process may wash away small amounts of these contaminants. However, by LC-MS analysis we were only able to confirm the presence of imazalil in the wastewater samples.

Heterotrophic bacteria measurements were performed in order to detect the presence of bacteria in the wastewater samples and confirm the removal of these organisms after the photocatalytic process.

4.2. Photocatalytic degradation of imazalil in synthetic industrial water

Fig. 1 shows the apparent first-order reaction rate constants determined for the degradation of imazalil (k_{IMZ}), as well as the percentage of mineralization after 120 min of irradiation for 50 mg L^{-1} of imazalil in deionized water and synthetic wastewater, at different pH values and a load of 1 g L^{-1} for the catalysts listed in Table 1. The synthetic wastewater contained 50 mg L^{-1} imazalil, 100 mg L^{-1} chloride (as NaCl), 300 mg L^{-1} sulphate (as $Al_2(SO_4)_3{\cdot}18H_2O$) and 20 mg L^{-1} calcium (as $Ca(OH)_2$), which simulates the composition generally found in the analyzed wastewater samples from the collaborating company.

It can be seen from Fig. 1 that the photocatalytic process in deionized water differs significantly from that in synthetic wastewater. Both mineralization and imazalil degradation were inhibited at acid pH values for the studies performed in synthetic wastewater and this inhibition increased significantly at pH 3.82.

To determine the extent to which each of the parameters in the synthetic water is responsible for inhibition of the degradation and mineralization of imazalil, the influence on the photocatalytic process of the most abundant components in real water was studied individually: chloride, bicarbonate and sulphate anions; and sodium, calcium and aluminium cations.

4.3. Effect of anions

The elimination of 50 mg L^{-1} imazalil was first carried out at different pH in the presence of 300 mg L^{-1} chloride (as NaCl), sulphate (as Na_2SO_4) or bicarbonate (as $NaHCO_3$) in order to determine the individual effect of each of these ions on the degradation and mineralization of imazalil (Fig. 2). In the experiments with bicarbonate ions, pH was maintained at 7 due to the instability of this ion at acid pH and always below 8.3 in order to inhibit the appearance of carbonate ions [20].

The amount of anions was then varied up to 1500 mg L^{-1} in order to evaluate the effect of higher anion concentrations on the photocatalytic treatment of 50 mg L^{-1} imazalil. Results showed that an

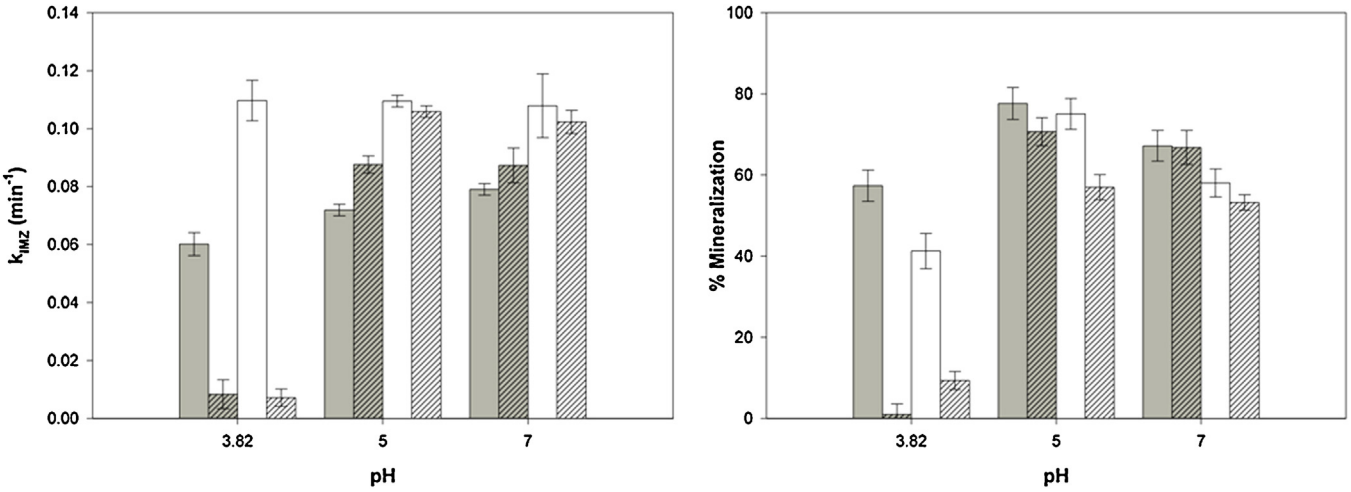

Fig. 1. Rate constant (left) and % mineralization (right) of imazalil after 120 min irradiation in deionized and synthetic industrial wastewater at different pH using different photocatalysts: Evonik P25 in deionized water ( ) and synthetic wastewater ( ), and EST-1023t in deionized water ( ) and synthetic wastewater ( ).

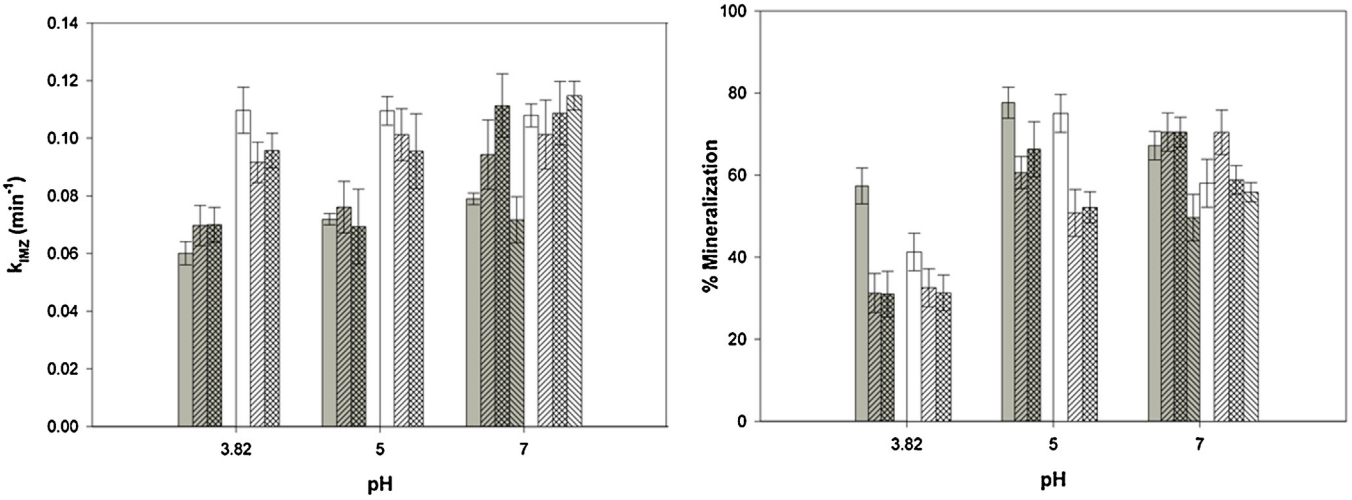

Fig. 2. Initial apparent degradation rate constant (left) and % Mineralization (right) of 50 mg L^{-1} imazalil after 120 min irradiation at different pH and for different water matrices and photocatalysts: Evonik P25 in deionized water ( ),+ Cl^- ( ),+ SO_4^{2-} ( ), +HCO_3^- ( ) and EST-1023t in deionized water ( ), +Cl^- ( ), +SO_4^{2-} ( ),+HCO_3^- ( ).

increase in anion concentrations above 300 mg L^{-1} has no significant additional negative effect on the mineralization process.

4.3.1. Effect of chloride

It can be seen from Fig. 2 that chloride anions have a negative effect on mineralization at pH < pH_{PZC} of the photocatalysts, that is, at pH 3 and 5. Mineralization inhibition is most marked at the lower pH value.

This can be explained, in general terms, by the adsorption of these anions on the photocatalyst surface at pH values where the catalyst is positively charged; that is below its pH_{PZC}, shown in Table 1 [21–26]. At acidic pH values, the adsorption of anions on the surface of the photocatalyst reduces the availability for the adsorption of intermediates, such as carboxylic acids, which are degraded by direct hole oxidation mechanism [27]. In alkaline solutions, such adsorption would be unlikely because of repulsive electrostatic forces. The adsorption of anions on the photocatalysts at acid pH values was confirmed by FTIR studies, as discussed in *Section 4.3.4*.

It should be noted that adsorption of imazalil under acidic conditions was negligible both in deionized water and in water containing chloride.

Many references have reported that chloride ions can scavenge h+ and •OH via the following general reactions [13,23,24,28–30]:

$$Cl^- + h^+ \rightarrow Cl^\bullet \quad (1)$$

$$Cl^- + {}^\bullet OH \rightarrow ClOH^{\bullet -} \quad (2)$$

$$ClOH^{\bullet -} + H^+ \rightarrow Cl^\bullet + H_2O \quad (3)$$

$$Cl^\bullet + Cl^- \rightarrow Cl_2^{\bullet -} \quad (4)$$

These radicals can be reduced back to chloride ions by electrons and therefore reduce the availability of holes, electrons and •OH [22]. Alternatively, chlorine and dichloride anion radicals can further react with organic compounds via addition/elimination reactions. Potential of chlorine (see Table 3) is similar to that of valence band holes [31–33]. However, we were unable to detect any new chlorinated intermediates by LCMS analysis for the elimination of imazalil in the presence of chloride ions.

Table 3
Redox potentials for some oxidizing species.

Redox pair	E° (V) vs. NHE	Reference
$Cl^\bullet/Cl^-$	2.47	[31]
$SO_4^{\bullet -}/SO_4^{2-}$	2.43	[33]
$CO_3^{\bullet -}$, H^+/HCO_3^-	1.78	[34]

Imazalil (m/z 297) has been reported to follow three degradation pathways. The first involves hydroxyl (or some other oxidizing species) attack on the ether to obtain product with m/z 257 [9,10,35]. The other two pathways involve the hydroxylation of imazalil before attack on the ether via the formation of product with m/z 331, which is rapidly transformed into m/z 313 and mainly into m/z 345 [10], as shown in Fig. 3. These degradation pathways are followed in a similar way by the two photocatalysts in this study: Evonik P25 and EST-1023t.

The presence of chloride ions in the photocatalytic system has shown to slow down the appearance of imazalil main intermediates m/z 257 and m/z 331. In addition, at acid pH the production of m/z 331 is reduced, and there seems to be an accumulation of m/z 257 (not shown). Therefore, chloride ions seem to inhibit the degradation of imazalil via direct hydroxylation and maybe promote the elimination of the compound through other pathways. The decrease in hydroxylated derivatives due to high concentrations of chloride has been described for the degradation of other compounds in the literature [29].

4.3.2. Effect of sulphate

The effects on the degradation and mineralization of imazalil caused by the addition of sulphate to the photocatalytic system were similar to those produced by the addition of chloride anions.

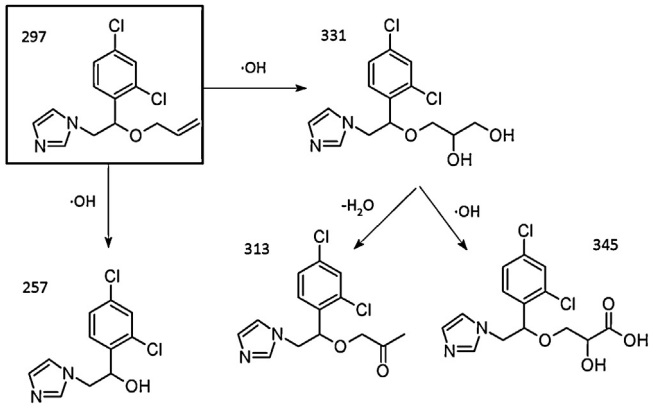

Fig. 3. Main photoproducts of imazalil. Degradation pathway.

It can be seen from Fig. 2 that sulphate ions lead to an inhibition in the mineralization of imazalil at acid pH, possibly due to the adsorption of the ions onto the photocatalysts and the scavenging of holes and •OH [13,25,26,36] according to the following reactions:

$$SO_4^{2-} + h^+ \rightarrow SO_4^{\bullet -} \quad (5)$$

$$SO_4^{2-} + {}^{\cdot}OH \leftrightarrow SO_4^{\bullet -} + OH^- \quad (6)$$

$$SO_4^{\bullet -} + e_{CB}^- \rightarrow SO_4^{2-} \quad (7)$$

When using Evonik P25 as photocatalyst, the apparent degradation rate constant increased slightly when sulphate was added. This may be because, even though the sulphate anion radical is less reactive than •OH, it may oxidize organic molecules. On the other hand, addition of SO_4^{2-} slightly increases the formation of hydroxyl radicals photolytically [25,26,37]. However, at pH < 7, $SO_4^{\bullet -}$ has been reported to be the predominant radical [38], while at neutral pH both $SO_4^{\bullet -}$ and •OH are responsible for the degradation of imazalil [39].

$S_2O_8^{2-}$ generates sulphate radical anions photolytically in aqueous solution [26,40]. A blank UV/$K_2S_2O_8$ experiment with imazalil and 1500 mg L^{-1} $K_2S_2O_8$ at pH 3.82 (no photolysis of imazalil) revealed that imazalil is slightly degraded by $SO_4^{\bullet -}$ with an apparent degradation rate constant of 0.023 min^{-1}.

Regarding LCMS analysis, similar results were obtained at pH 7 in presence of sulphate ions to those observed when chloride ions were added. In this sense, hydroxyl photoproducts become scarcer than in deionized water. Studies at pH 3.82 revealed very small amounts of photoproducts, indicating that a different mechanism is responsible for the degradation under these conditions. Additionally, these results agree with a recent study [39], in which the authors confirm the opening of the imidazole ring to be the main degradation pathway of imazalil in presence of $K_2S_2O_8$ via electron transfer induced by sulfate radicals.

4.3.3. Effect of bicarbonate

Precaution needs to be taken when working with bicarbonate because of its unstable equilibrium with the atmosphere. For this reason, the working pH with this anion was set at 7 ± 0.5.

Bicarbonate ions have been reported to be h^+ and radical scavengers [12,22,23,41], according to the following reactions:

$$HCO_3^- + h^+ \rightarrow HCO_3^{\bullet -} \quad (8)$$

$$HCO_3^- + {}^{\bullet}OH \rightarrow CO_3^{\bullet -} + OH^- \quad (9)$$

It can be seen from Fig. 2 that this ion produces a negative effect on the apparent degradation rate constant of imazalil and its mineralization when using photocatalyst Evonik P25. This effect is not observed when using EST-1023t, probably due to the higher capacity of the lab-made photocatalyst to produce •OH radicals [42].

Adsorption experiments in the absence of imazalil revealed that small amounts of HCO_3^- may be adsorbed onto the photocatalysts. This was confirmed by FTIR studies, as discussed in *Section 4.3.4*. However, the concentration of bicarbonate ions throughout the photocatalytic degradation of imazalil significantly decreased, as shown in Fig. 4. This may indicate the reactivity of the carbonate radical with the molecules of imazalil in detriment of imazalil degradation.

On the other hand, as can be seen in Fig. 5, bicarbonate ions enhanced the adsorption of imazalil and UV–Vis spectra did not reveal complex formation between imazalil and these ions. This is attributed to the surface modification that bicarbonate ions produce on the photocatalyst (as discussed in *Section 4.3.4*): an increase in surface hidrophobicity enhanced imazalil adsorption at pH 7. This increased adsorption of imazalil, however, does not seem to influence the photooxidation of the contaminant [10].

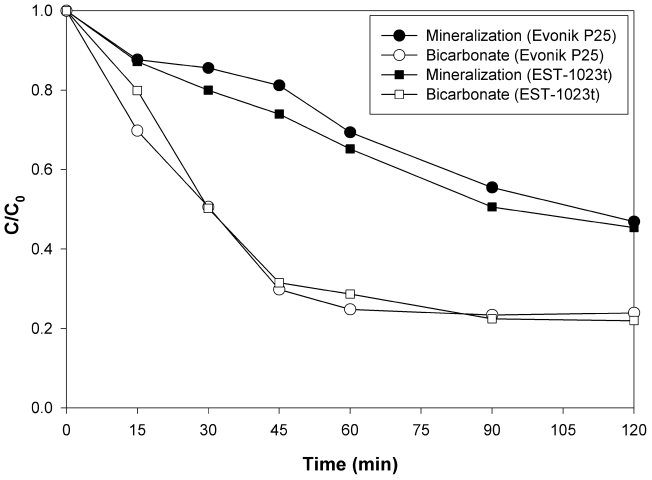

Fig. 4. Mineralization and bicarbonate ion reduction during the photocatalytic treatment of 50 mg L^{-1} imazalil in presence of 100 mg L^{-1} bicarbonate at a constant pH = 7.3 ± 0.5 using the photocatalysts Evonik P25 and EST-1023t.

It should be noted that at pH 7 the amount of imazalil adsorbed on the photocatalyst was not modified by the presence of chloride or sulphate ions (Fig. 5).

4.3.4. FTIR studies

In Fig. 6, the band observed at 3698 cm^{-1} is attributed to isolated hydroxyl groups (OH_{iso}). These groups indicate the presence on the surface of the photocatalyst of oxygen vacancies or defects [43,44]. The band that in all spectra was observed at 1640 cm^{-1} is attributed to the water bending mode ($\nu 2$). The broad band between 3650 and 3000 cm^{-1} is attributed to the asymmetrical ($\nu 3$) and symmetrical ($\nu 1$) vibration modes of water [45]. The shape and relative intensity of the bands attributed to vibrations $\nu 3$ and $\nu 1$ with respect to the corresponding vibration $\nu 2$ is different depending on the pH and the presence of different ions.

At pH 7 the spectrum of Evonik P25 with adsorbed water is very similar to that of pure water; that is, the bands attributed to vibrations $\nu 3$ and $\nu 1$ appear very close, which is due to a strong effect of hydrogen bonding [45]. At pH 3 the bands allocated to vibrations $\nu 3$ and $\nu 1$ are broader and show a much lower relative intensity compared to $\nu 2$ than at pH 7. Moreover, the broad band at pH 3 could be divided into four bands: the two bands present

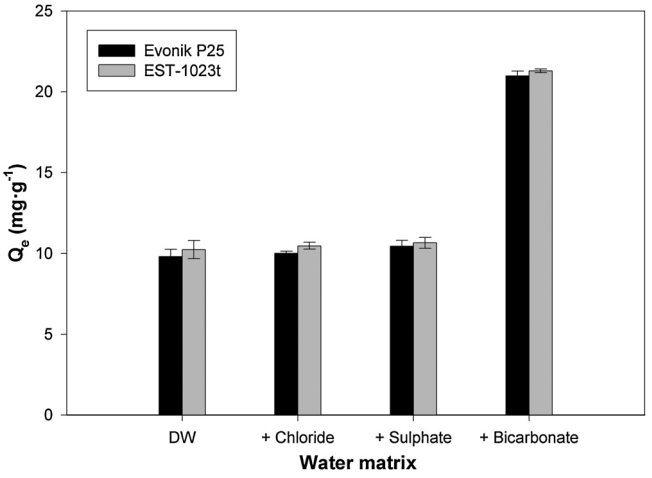

Fig. 5. Adsorption capacity (q_e) of imazalil on the photocatalysts Evonik P25 and EST-1023t at pH 7 in different water matrices. Anions concentrations employed have been of 300 mg L^{-1}. DW stands for deionized water.

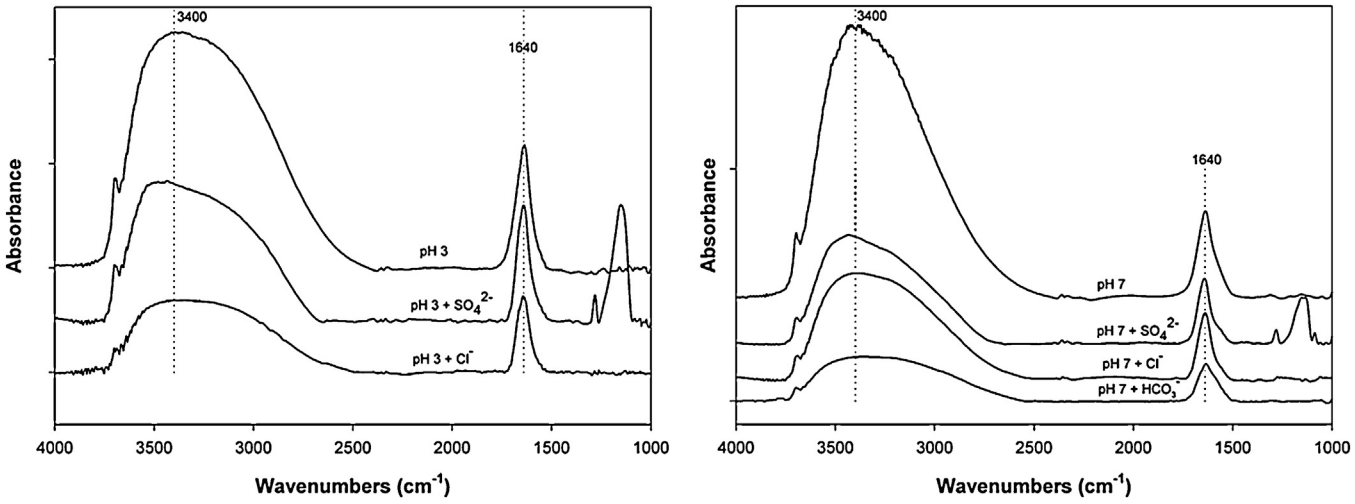

Fig. 6. FTIR spectra from interaction of Evonik P25 after adsorption equilibrium at different pH with 300 mg L^{-1} Cl^- (as NaCl), 300 mg L^{-1} SO_4^{2-} (as Na_2SO_4), 300 mg L^{-1} HCO_3^- (as $NaHCO_3$) and the photocatalyst alone.

at lower wavenumbers are attributable to vibrations $\nu 3$ and $\nu 1$, corresponding to water molecules strongly bound to the surface of the catalyst through Ti-OH_2 type interaction given the similarity of the relative intensities of these bands with vibration $\nu 2$. Meanwhile, the bands at higher wavenumbers may be attributed to vibrations $\nu 3$ and $\nu 1$ which represent isolated molecules interacting via hydrogen bonds [46]. That is, the main difference that can be observed in the spectra of P25 at pH 7 and 3 is that at the higher pH more layers of water appear to be adsorbed onto the catalyst surface.

A common characteristic can be observed in the IR-spectra from the interaction of the photocatalyst with chloride and sulphate at pH 3 and bicarbonate ions at pH 7: the water layer on the surface seems to decrease; that is, the adsorbed water molecules are more isolated. This can be related to a higher aggregation of catalyst particles for increasing ionic strength [47], which can affect the photoactivity. Moreover, this phenomenon is only observed for the conditions in which the photocatalytic mineralization of imazalil is hindered. Therefore, we can affirm that these anions, under the mentioned pH conditions, produce deactivation of the catalyst to water adsorption, and thus inhibit the photocatalytic process, in agreement with [23].

4.4. Effect of cations

The elimination of 50 mg L^{-1} imazalil was tested at different pH in the presence of 300 mg L^{-1} sulphate salts of different cations (Na_2SO_4, $CaSO_4{\cdot}2H_2O$ and $Al_2(SO_4)_3{\cdot}18H_2O$) in order to determine the individual effect of each of these metal cations on the degradation and mineralization of imazalil. Results are shown in Fig. 7.

No discernible effects were observed at pH 7 when these cations were added to the solution. It should be noted that at pH 7 aluminium precipitates as aluminium hydroxide and was removed from the solution. However, at acid pH the presence of aluminium in solution hinders both imazalil degradation and mineralization.

4.4.1. Effect of aluminium

Due to the strong inhibition produced by the presence of dissolved aluminium on the degradation and mineralization of imazalil, we decided to study this phenomenon in greater depth.

The amount of dissolved aluminium was measured by GFAAS at different pH values for a 300 mg L^{-1} sulphate solution (as $Al_2(SO_4)_3{\cdot}18H_2O$). At pH 3.82, 5 and 7 the dissolved aluminium was 56.37 mg L^{-1}, 328.50 μg L^{-1} and 73.42 μg L^{-1}, respectively. However, it can be seen from Table 2 that the maximum aluminium

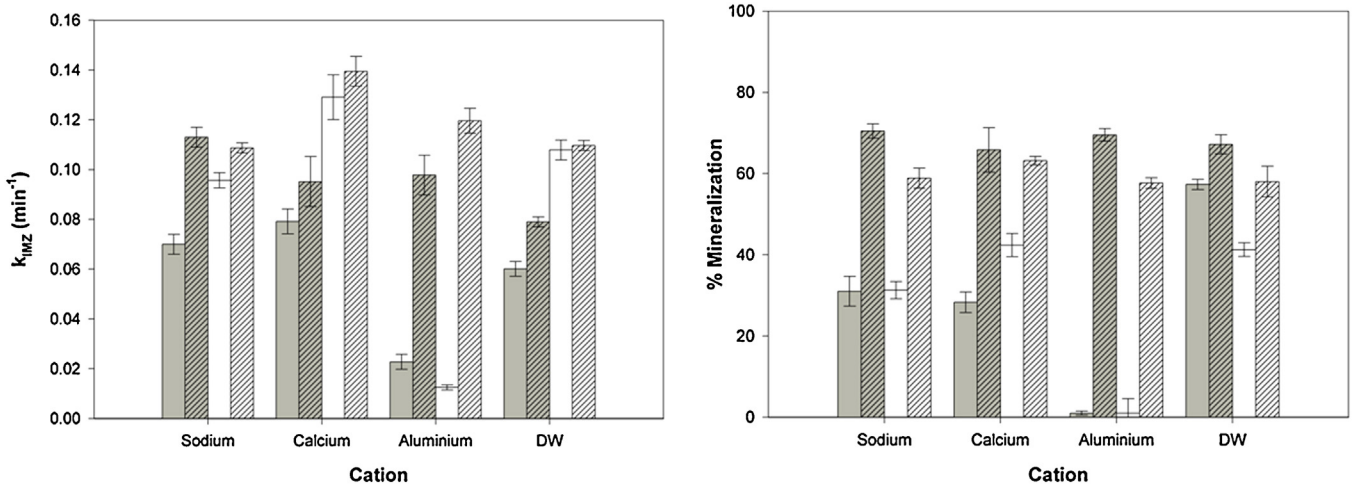

Fig. 7. Initial apparent degradation rate constant (left) and % mineralization (right) of 50 mg L^{-1} imazalil after 120 min irradiation with photocatalysts Evonik P25 at pH 3.82 ( ) and 7 ( ); and EST-1023t at pH 3.82 ( ) and 7 ( ) in presence of different cations (for sulphate salts).

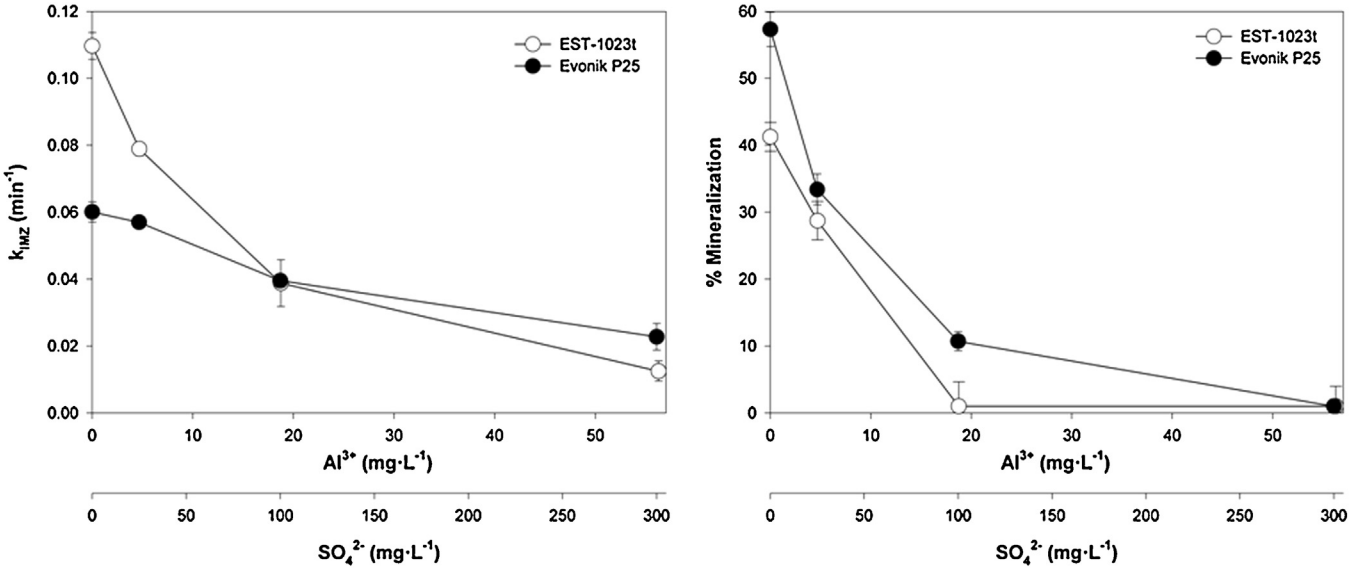

Fig. 8. Initial apparent degradation rate constant (left) and % Mineralization (right) of 50 mg L^{-1} imazalil at pH 3.82 and after 120 min irradiation with photocatalysts Evonik P25 (-●-) and EST-1023t (-○-) in presence of different aluminium concentrations (for sulphate salt).

concentration found in the wastewater sample was 4.04 mg L^{-1}. The concentration of dissolved aluminium was varied in order to study the effect of this cation on the elimination of imazalil.

It can be seen from Fig. 8 that the elimination and mineralization of imazalil were affected by the presence of aluminium even at concentrations as low as 5 mg L^{-1}. It has been shown that at pH values below the PZC of the photocatalysts, although both Al(III) and TiO_2 surface are positively charged, Al(III) adsorption occurs [48]. The FTIR spectra shown in Fig. 9a confirm a reduction in isolated hydroxyl groups (band at 3698 cm^{-1}) when Al(III) is adsorbed on the photocatalyst, with this effect increasing for lower pH values. The isolated hydroxyl groups are usually present at vertices and defects on the catalyst surface and are considered to be the most basic and photoactive groups [49]. For this reason, the adsorption of Al(III) on these groups hinders the photocatalytic degradation of imazalil. Although the references are scarce, the presence of Al(III), either adsorbed on the photocatalyst or on doped-TiO_2 has been reported to have a detrimental effect on the photodegradation of compounds that follow phenol-type mechanisms [50,51], such as imazalil.

The addition of Al(III) had a similar effect in EST-1023t and in Evonik P25 when considering FTIR studies. However, the reduction of isolated hydroxyl groups, and consequently hydroxyl radicals, due to dissolved aluminium, had a more significant detrimental effect on the initial apparent degradation rate constant of imazalil when using EST-1023t.

Additionally, ammonia interaction with the catalyst surface was studied in the presence and absence of dissolved Al(III), in order to determine the presence and modification of Lewis or Brönsted acid centres. Lewis acid centres are characterized by bands present between 1215 and 1000 cm^{-1}, and are stronger at higher band wavelengths. Accordingly, strong Lewis acid centres (SLAC, 1215–1180 cm^{-1}) and weak Lewis acid or physisorption centres (WLAC, 1150–1000 cm^{-1}) can be found. Brönsted acid centres (BAC) are characterized by a band centered at 1460–1430 cm^{-1}. When the molecule interaction occurs simultaneously at strong

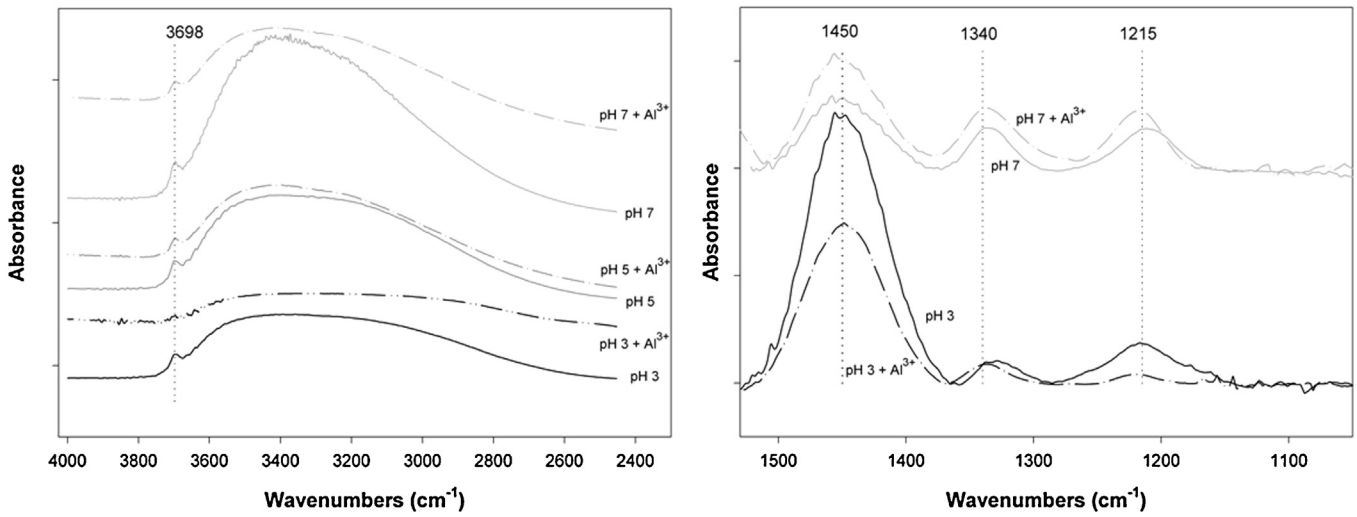

Fig. 9. FTIR spectra in the hydroxyl group region (left) and from the interaction of NH_3 (right) with Evonik P25 at different pH and in presence or absence of dissolved aluminium.

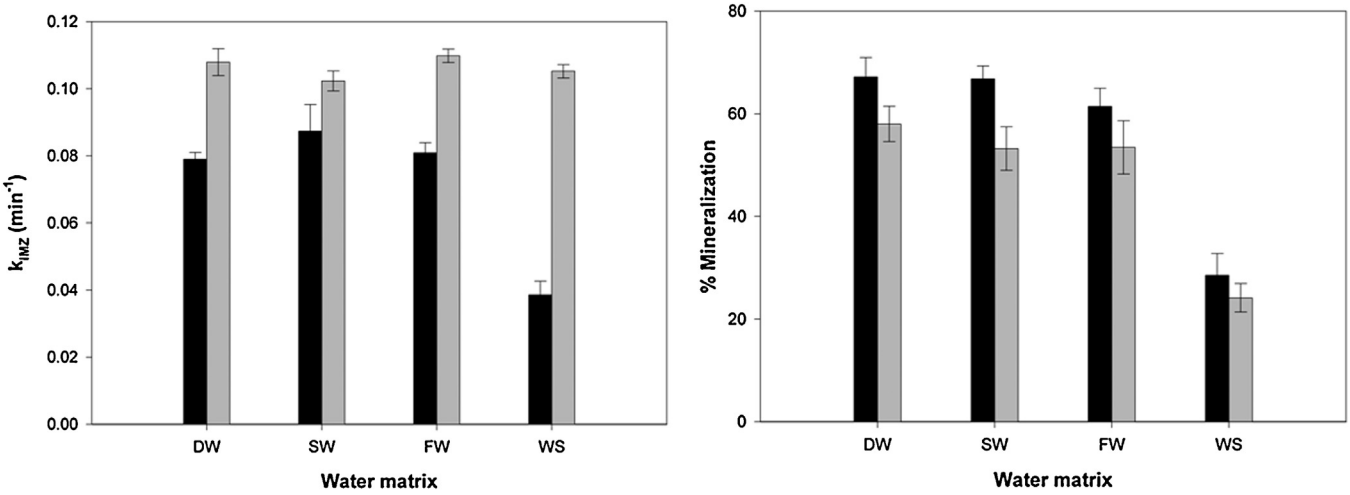

Fig. 10. Apparent degradation rate constant (left) and % mineralization of imazalil in different water matrices at pH 7 using two photocatalysts: Evonik P25 (■) and EST-1023t (▭). DW represents deionized water, SW synthetic saline water as described in section 4.2, FW filtered industrial wastewater and WS the supernatant of industrial wastewater.

Lewis acid and Brönsted acid centres, it breaks to give breaking centre bands between 1340 and 1320 cm^{-1} [52,53].

It can be seen from Fig. 9b that in the presence of Al(III) the bands corresponding to Lewis acid centres and to species produced by the split of NH_3 at the breaking centres appear at higher wavenumbers (1340 and 1215 cm^{-1}, respectively) and with higher relative intensities (only at pH 3) than those of Evonik P25 alone. This confirms the creation of strong Al(III) Lewis acid centres in the photocatalyst, which is consistent with previous references [54]. Thus, the adsorption of oxygen, and the consequent production of the $O_2^{\bullet -}$ species, is probably enhanced by the interaction of Al(III) [51]. From the low initial apparent degradation rate constants yielded in presence of Al(III), it is concluded that this oxidizing species is not crucial in the photocatalytic elimination of imazalil.

4.4.2. Effect of calcium and sodium

Calcium and sodium ions have a very similar effect on imazalil degradation and mineralization (Fig. 7). These cations do not apparently influence the process, and the decrease in mineralization observed at acid pH is a consequence of the sulphate counter-ions present in the water matrix.

The ability of the TiO_2 photocatalyst to undergo photoinduced electron transfer to adsorbed species on its surface depends on the fact that the potential level of the acceptor species is thermodynamically required to be more positive than the conduction band potential of the photocatalyst. Accordingly, the potential level of the donor species needs to be more negative than the valence band position in order to donate an electron to the vacant hole. These band edge positions are influenced by the pH of the electrolyte as well as the structural characteristics of the semiconductor [55]. Therefore, the effect of cations on the photocatalytic activity is strongly dependant on the standard reduction potential of the metal.

For different TiO_2 and at different pH, the potential for the valence band is ≈2.39–2.80 V vs. NHE, and for the conduction band is ≈0.4–0.52 V vs. NHE [14,30,56,57]. The standard reduction potentials for the metals discussed are −2.71 V vs. NHE for $E^{\circ}(Na^{+}/Na)$ and −2.87 V vs. NHE for $E^{\circ}(Ca^{2+}/Ca)$. A comparison of these values with those from the band edge potentials of TiO_2 indicates that these cations are not likely to interact with the photogenerated holes and electrons. This may explain the negligible effect of these ions on the photocatalytic process.

4.5. Industrial wastewater treatment

Finally, the elimination and mineralization of 50 mg L^{-1} imazalil was performed in a real wastewater sample (see Table 2). Results are shown in Fig. 10.

It can be observed that at pH values around 7, the effect of anions was negligible for filtered wastewater samples. However, when using the wastewater supernatant as water matrix the apparent degradation rate constant was strongly affected for Evonik P25 and mineralization was significantly hindered for both the commercial photocatalyst and the lab-made EST-1023t. This may be attributed to the presence of bacteria in the supernatant of industrial wastewater.

Inactivation of bacteria is a known application of heterogeneous photocatalysis that has been studied by many authors [23,58–61] and has been attributed mainly to the concentration of •OH radicals [58]. In this study, the initial bacteria count was 2×10^4 CFU·100 mL^{-1}, and these disappeared completely after 15 min irradiation when using photocatalyst EST-1023t and after 30 min for Evonik P25. The ability of EST-1023t to produce more hydroxyl radicals may be the reason for the faster elimination of bacteria and, consequently, the lower effect of the presence of these bacteria on the apparent degradation rate constant of imazalil.

Despite this, mineralization of imazalil was inhibited for both photocatalysts due to bacteria. The inactivation of bacteria produces intermediate metabolites that are also degraded [62] and compete with the degradation of imazalil photoproducts. Moreover, remaining bacteria may compete with the adsorption and degradation of imazalil photoproducts.

5. Conclusions

Several water-matrix effects on the photocatalytic degradation and mineralization of imazalil were studied. Anions such as sulphate and chloride were shown to adsorb onto the TiO_2 photocatalysts at acid pH and thus inhibit the mineralization of the contaminant. A similar effect was produced by bicarbonate ions at pH 7.

As for cations, dissolved aluminium was shown to strongly hinder the photocatalytic decontamination of imazalil due to its adsorption and subsequent modification of the photocatalyst surface, as concluded from FTIR spectra.

Bacteria present in industrial wastewaters were rapidly removed by the UV/TiO_2 system, but were also seen to have a detrimental effect on the removal of imazalil.

Similar TiO_2 photocatalysis efficiencies for the treatment of imazalil present in a deionized water-matrix and in industrial wastewater were only obtainable when the wastewater (was filtered and) was at pH values where adsorption of the most abundant ions is prevented, that is, at pH 7.

Acknowledgements

We thank the Universidad de Las Palmas de Gran Canaria for the funding through the PhD Grant Program, the Banana Producers Association (Spain) and MINECO (Ministry of Economy and Competitiveness, Government of Spain) for funding projects NANOBAC (IPT-2011-1113-310000) and 2010-3E-UNLP10-3E-MINECO-726.

References

[1] DOUE, Reg. 1107/2009/EC, L309 (2009) 1–48.
[2] DOUE, Reg. 396/2005/EC, L70 (2005) 1–16.
[3] D.J. Hamilton, Á. Ambrus, R.M. Dieterle, A.S. Felsot, C.A. Harris, P.T. Holland, A. Katayama, N. Kurihara, J. Linders, J. Unsworth, S.S. Wong, Pure Appl. Chem. 75 (2003) 1123–1155.
[4] COPLACA, Pudrición de corona en el plátano canario, 2004.
[5] J. Araña, C. Garriga, C. Fernández Rodríguez, J.A. Herrera Melián, J.A. Ortega Méndez, J.M. Doña Rodríguez, J. Pérez Peña, Chemosphere 71 (2008) 788–794.
[6] Y. Tang, G. Zhang, C. Liu, S. Luo, X. Xu, L. Chen, B. Wang, J. Hazard. Mater. 252–253 (2013) 115–122.
[7] J.A. Arroyave Rojas, L.F. Garcés Giraldo, A.F. Cruz Castellanos, Rev. Lasallista Invest. 3 (2006) 19–24.
[8] J.A. Arroyave Rojas, L.F. Garcés Giraldo, A.F. Cruz Castellanos, Rev. Lasallista Invest. 4 (2007) 1–7.
[9] R. Hazime, C. Ferronato, L. Fine, A. Salvador, F. Jaber, J.M. Chovelon, Appl. Catal. B: Environ. 126 (2012) 90–99.
[10] D.E. Santiago, J.M. Doña-Rodríguez, J. Araña, C. Fernández-Rodríguez, O. González-Díaz, J. Pérez-Peña, Adrián M.T. Silva, Appl. Catal. B: Environ. 138–139 (2013) 391–400.
[11] A. Afzal, P. Drzewicz, J.W. Martin, M.G. El-Din, Sci. Total Environ. 426 (2012) 387–392.
[12] W. Zhang, Y. Li, Y. Su, K. Mao, Q. Wang, J. Hazard. Mater. 215–216 (2012) 252–258.
[13] P.S. Yap, T.T. Lim, Appl. Catal. B: Environ. 101 (2011) 709–717.
[14] V. Brezova, A. Blaikova, E. Borosova, M. Ceppan, R. Fiala, J. Mol. Catal. A: Chem. 98 (1995) 109–116.
[15] E.I. Seck, J.M. Doña-Rodríguez, C. Fernández-Rodríguez, D. Portillo-Carrizo, M.J. Hernández-Rodríguez, O.M. González-Díaz, J. Pérez-Peña, Solar Energy 87 (2013) 150–157.
[16] R.M. Cavalcantea, D.M. Lima, G.M. Fernandes, W.C. Duaví, Talanta 93 (2012) 212–218.
[17] BOC, Decreto 82/1999, 73 (1999) 8382–8436.
[18] BOE, Real Decreto 1620/2007, 294 (2007) 50639–50661.
[19] Registro de Productos Fitosanitarios, Spain, Ministerio de Medio Ambiente y Medio Rural y Marino, 2013.
[20] W.K. Dodds, M.R. Whiles, Freshwater Ecol.: Concepts Environ. Appl. Limnol. (2010) 324–328.
[21] C. Hu, J.C. Yu, Z. Hao, P.K. Wong, Appl. Catal. B: Environ. 46 (2003) 35–47.
[22] A. Lair, C. Ferronato, J.M. Chovelon, J.M. Herrmann, J. Photochem. Photobiol. A Chem. 193 (2008) 193–20323.
[23] A.G. Rincón, C. Pulgarin, Appl. Catal. B: Environ. 51 (2004) 283–302.
[24] K.H. Wang, Y.H. Hsieh, M.Y. Chou, C.Y. Chang, Appl. Catal. B: Environ. 21 (1999) 1–8.
[25] N. Kashif, F. Ouyang, J. Environ. Sci. 21 (2009) 527–533.
[26] S. Ahmed, M.G. Rasul, R. Brown, M.A. Hashib, J. Environ. Manag. 92 (2011) 311–330.
[27] Y. Chen, S. Yang, K. Wang, L. Lou, J. Photochem. Photobiol. 172 (2005) 47–54.
[28] M. Sökmen, A. Özkan, J. Photochem. Photobiol. A: Chem. 147 (2002) 77–81.
[29] C. Sirtori, A. Agüera, W. Gernjak, S. Malato, Water Res. 44 (2010) 2735–2744.
[30] X.Y. Yu, J.R. Barker, J. Phys. Chem. A 107 (2003) 1325–1332.
[31] Ruixia Yuan, Sadiqua N. Ramjaun, Zhaohui Wang, Jianshe Liu, Chem. Eng. J. 192 (2012) 171–178.
[32] D. Wang, Y. Li, G.L. Puma, C. Wang, P. Wang, W. Zhang, Q. Wang, Chem. Commun. 49 (2013) 10367–10369.
[33] R.E. Huie, C.L. Clifton, P. Neta, Int. J. Radiat. Appl. Instrument. Part C. Radiat. Phys. Chem. 38 (1991) 477–481.
[34] O. Augusto, M.G. Bonini, A.M. Amanso, E. Linares, C.C.X. Santos, S.L. de Menezes, Free Radic. Biol. Med. 32 (2002) 841–859.
[35] A.K. Genena, Tratamento de Efluente Agroindustrial Contend Compostos Persistentes por meio dos Processos de Coagulaçao-floculaçao, Fenton, Foto-Fenton, Foto-peroxidaçao e Ozonizaçao. Universidade Federal de Santa Catarina. Florianópolis, 2009.
[36] W. Xhang, T. An, M. Cui, G. Sheng, J. Fu, J. Chem. Technol. Biotechnol. 80 (2005) 223–229.
[37] H. Sheng, Q. Li, W. Ma, H. Ji, C. Chen, J. Zhao, Appl. Catal. B: Environ. 138–139 (2013) 212–218.
[38] C. Liang, H.W. Su, Ind. Eng. Chem. Res. 48 (2009) 5558–5562.
[39] R. Hazime, Q.H. Nguyen, C. Ferronato, A. Salvador, F. Jaber, J.M. Chovelon, Appl. Catal. B: Environ. 144 (2014) 286–291.
[40] R. Hazime, Q.H. Nguyen, C. Ferronato, T.K.X. Huynh, F. Jaber, J.M. Chovelon, Appl. Catal. B: Environ. 132–133 (2013) 519–526.
[41] L. Hu, P.M. Flanders, P.L. Miller, T.J. Strathmann, Water Res. 41 (2007) 2612–2626.
[42] L.M. Pastrana-Martínez, J.L. Faria, J.M. Doña-Rodríguez, C. Fernández-Rodríguez, A.M.T. Silva, Appl. Catal. B: Environ. 113–114 (2012) 221–227.
[43] J. Trimboli, M. Mottern, H. Verweij, P.K. Dutta, J. Phys. Chem. B 110 (2006) 5647–5654.
[44] C. Deiana, E. Fois, S. Coluccia, G. Martra, J. Phys. Chem. C 114 (2010) 21531–21538.
[45] H.A. Al-Abadleh, V.H. Grassian, Langmuir 19 (2003) 341–347, 46.
[46] L. Cammarata, S.G. Kazarian, P.A. Salterb, T. Welton, Phys. Chem. Chem. Phys. 3 (2001) 5192–5200.
[47] P. Fernández-Ibáñez, J. Blanco, S. Malato, F.J. de las, Nieves, Water Res. 37 (2003) 3180–3188, 48.
[48] G.R. Weise, T.W. Healy, J. Colloid Interface Sci. 51 (1975) 434–442.
[49] J. Araña, A. Peña Alonso, J.M. Doña Rodríguez, G. Colón, J.A. Navío, J. Pérez Peña, Appl. Catal. B: Environ. 89 (2009) 204–213.
[50] V. Brezová, A. Blazková, L. Karpinský, J. Grosková, B. Havlínová, V. Jorík, M. Ceppan, J. Photochem. Photobiol. A: Chem. 109 (1997) 177–183.
[51] M.I. Franch, J. Perala, X. Domènech, R.F. Howe, J.A. Ayllón, Appl. Catal. B: Environ. 55 (2005) 105–113.
[52] J. Araña, D. Portillo-Carrizo, J.A. Ortega Méndez, J.A. Herrera Melián, J.M. Doña Rodríguez, J. Pérez-Peña, O. González Díaz, J. Photochem. Photobiol. A 249 (2012) 61–69.
[53] G. Martra, Appl. Catal. A: Gen. 200 (2000) 275–285.
[54] K. Hadjiivanov, Appl. Surf. Sci. 135 (1998) 331–338.
[55] C. Lahousse, F. Mauge, J. Bachelier, J.C. Lavalley, J. Chem. Soc. Faraday Trans. 91 (1995) 2907–2912.
[56] A.L. Linsebigler, G. Lu, J.T. Yates, Chem. Rev. 95 (1995) 735–758.
[57] A. Fujishima, T.N. Rao, D.A. Tryk, J. Photochem. Photobiol. C Photochem. Rev. 1 (2000) 1–21.
[58] M. Cho, H. Chung, W. Choi, J. Yoon, Water Res. 38 (2004) 1069–1077.
[59] S. Sontakke, J. Modak, G. Madras, Appl. Catal. B: Environ. 106 (2011) 453–459.
[60] Z. Huang, P.C. Maness, D.M. Blake, E.J. Wolfrum, S.L. Smolinski, W.A. Jacoby, J. Photochem. Photobiol. A: Chem. 130 (2000) 163–170.
[61] M. Planchona, R. Ferrari, F. Guyot, A. Gélabert, N. Menguy, C. Chanéac, A. Thill, M.F. Benedetti, O. Spalla, Colloids Surf. B: Biointerfaces 102 (2013) 158–164.
[62] D. Gumy, C. Morais, P. Bowen, C. Pulgarin, S. Giraldo, R. Hajdu, J. Kiwi, Appl. Catal. B: Environ. 63 (2006) 76–84.